doi:10.1017/S1431927622007036
Microsc. Microanal. 28 (Suppl 1), 2022

Disentangling Exciton Linewidth Broadening Factors in Transition Metal Dichalcogenide Monolayer with Electron Energy Loss Spectroscopy

Fuhui Shao[1], Steffi Y. Woo[1], Nianjheng Wu[1,2], Robert Schneider[3], Andrew J. Mayne[2], Steffen Michaelis[3], Ashish Arora[3,7], Benjamin J. Carey[3], Johann A. Preuß[3], Noémie Bonnet[1], Cecilia Mattevi[4], Kenji Watanabe[5], Takashi Taniguchi[6], Rudolf Bratschitsch[3] and Luiz H. G. Tizei[1*]

[1.] Université Paris-Saclay, CNRS, Laboratoire de Physique des Solides, Orsay, France.
[2.] Université Paris-Saclay, Institut des Sciences Moléculaires d'Orsay, Orsay, France.
[3.] Institute of Physics and Center for Nanotechnology, University of Münster, Münster, Germany.
[4.] Department of Materials, Imperial College London, London, UK.
[5.] Research Center for Functional Materials, National Institute for Materials Science, Tsukuba, Japan.
[6.] International Center for Materials Nanoarchitectonics, National Institute for Materials Science, Tsukuba, Japan.
[7.] Indian Institute of Science Education and Research, Pune, India.
* Corresponding author: luiz.galvao-tizei@universite-paris-saclay.fr

Monolayer two-dimensional transition metal dichalcogenides (TMDs) have invoked great interest for potential applications because of their strong light-matter interactions and direct energy gap. However, the external environment heavily influences the optical properties of TMD monolayers. Encapsulating TMDs in *h*-BN is recognized as the most effective way to preserve their intrinsic optical properties [1,2], and to obtain narrow excitonic linewidths. It has been proven that *h*-BN encapsulation can reduce the roughness of graphene from 114 ± 1 to 12 ± 5 pm [3]. Besides roughness, surface protection [1], charge disorder [2], and variations of dielectric environment [4] are also believed to be key factors that could induce inhomogeneous excitonic linewidth broadening of TMDs. However, no such study has comprehensively compared and disentangled the various proposed factors that contribute to excitonic linewidth broadening exists, because few techniques can address all factors single-handedly.

In order to explore the role of these factors, we investigated the roughness and absorption behavior by electron energy loss spectroscopy (EELS) of WS_2 monolayers either supported or encapsulated by two different nanosheets (*h*-BN and Si_3N_4) in a scanning transmission electron microscope (STEM) [5]. Using this technique, the factors leading to exciton absorption linewidth inhomogeneity can be ranked in increasing order of importance: monolayer roughness, surface cleanliness, and substrate induced charge trapping. In Fig. 1., the EELS spectra of WS_2 monolayers in different configurations are illustrated.

Experiments were done on the ChromaTEM microscope, a modified Nion HERMES 200 equipped with an electron monochromator. The electron beam energy is set at 60 keV with a spread down to below 10 meV. The convergence half-angles for the EELS and diffraction measurements are 10 mrad and 1 mrad. Roughness was measured with the sample tilted with respect to the electron beam from 0 to 385 mrad as shown in Fig. 2, which is similar to previous experiments for graphene [3,6]. Corrugated monolayers are expected to show diffraction spots blurring as the tilt angle increases, whereas a flat monolayer does not. Additionally, numerical calculations for the diffraction patterns under different roughnesses are performed in QSTEM [7] to ascertain the corrugation of the monolayers in each configuration [8].

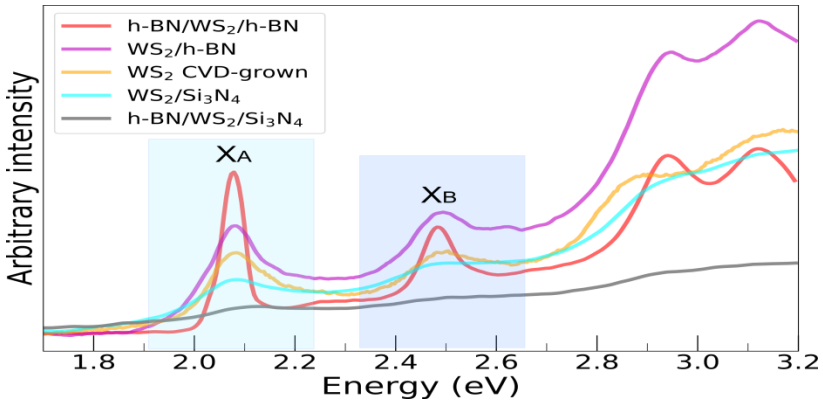

Figure 1. EELS spectra of WS_2 monolayers in various configurations at 110 K. The linewidth of the A exciton in increasing order is: *h*-BN encapsulated, *h*-BN supported, freestanding CVD-grown, Si_3N_4 supported and Si_3N_4/*h*-BN encapsulated WS_2 monolayers.

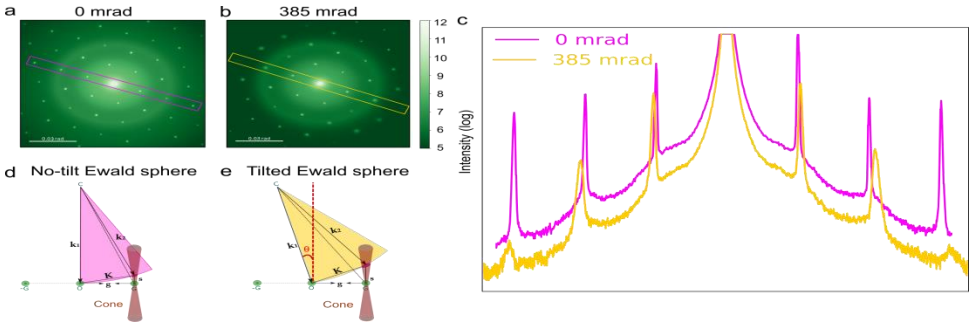

Figure 2. (a) and (b) are the diffraction patterns of a WS_2 monolayer on a 15-nm Si_3N_4 membrane, corresponding to the reciprocal space of a corrugated monolayer and Ewald sphere geometry in (d) and (e). The intensity profiles of the diffraction spots are plotted in (c), which are indicated in (a) and (b) by the purple and yellow box.

References:

[1] F Cadiz et al., Phys. Rev. X **7** (2017), p. 021026. doi: 10.1103/PhysRevX.7.021026
[2] OA Ajayi et al., 2D Mater. **4** (2017), p. 031011. doi: 10.1088/2053-1583/aa6aa1
[3] JD Thomsen et al., Phys. Rev. B **96** (2017), p. 014101. doi: 10.1103/PhysRevB.96.014101
[4] A Raja et al., Nat. Nanotechnol. **14** (2019), p. 832. doi: 10.1038/s41565-019-0520-0
[5] F Shao et al., ArXiv (2022). doi: arXiv:2202.04483
[6] JC Meyer et al., Nature **446** (2007), p. 60. doi: 10.1038/nature05545
[7] C. T. Koch in "Determination of core structure periodicity and point defect density along dislocations" (2002) Arizona State University.
[8] This project has been funded in part by the National Agency for Research under the program of future investment TEMPOS-CHROMATEM (reference no. ANR-10-EQPX-50) and the MAGMA research grant (ANR-16-CE09-0027), and the JCJC grant SpinE (reference no. ANR-20-CE42-0020) and by the European Union's Horizon 2020 research and innovation programme under grant agreement No. 823717 (ESTEEM3) and 101017720 (EBEAM). This work has been supported by Region Île-de-France in the framework of DIM SIRTEQ.

https://doi.org/10.1017/S1431927622007036 Published online by Cambridge University Press